Nuclear magnetic resonance studies of highly oriented liquid crystalline copolyesters

R. A. Allen and I. M. Ward*
IRC in Polymer Science and Technology, The University of Leeds, Leeds LS2 9JT, UK
(Received 6 December 1989; revised 14 February 1990; accepted 16 February 1990)

Highly oriented copolymers prepared from 4-hydroxybenzoic acid and 2-hydroxy-6-naphthoic acid and having monomer ratios of 73:27 and 30:70 have been studied by modelling the second moment anisotropies of their nuclear magnetic resonance proton lineshapes. At −100°C the results are consistent with chains of immobile aromatic rings placed on a pseudo-hexagonal lattice. As temperature is increased the changes in the second moment anisotropies are accounted for by allowing first the phenyl and then the naphthalene rings to acquire rapid rotational motion. It is also necessary to introduce an accompanying increase in the distribution of chain axes about the sample draw direction. This may be due to increasing chain motion.

(Keywords: nuclear magnetic resonance; liquid crystalline copolyesters)

INTRODUCTION

Much research activity continues to be directed towards an understanding of the structure and chain motion in copolymers formed from 4-hydroxybenzoic acid (HBA) and 2-hydroxy-6-naphthoic acid (HNA). The relationship between structure and properties of this class of materials has been reviewed by Davies and Ward[1]. X-ray diffraction studies[2] have analysed the liquid crystalline nature of these materials, whereas dynamic relaxation measurements[3] have shown that the mechanical properties are dependent on the degree of rotational freedom of the HBA and HNA groups. We have also used nuclear magnetic resonance (n.m.r.) spectroscopy to investigate further the structure of the HBA:HNA copolymers[4]. This technique is capable of probing the local environments of nuclei in the material. We have previously used a Varian DP60 continuous wave (CW) spectrometer operating at 60 MHz to observe the proton broadline spectrum from a material with a HBA:HNA monomer ratio of 73:27. The variation of the second moments with temperature and sample orientation has been investigated and computer models used to simulate the n.m.r. results. Experimental results at −60, 20 and 140°C were explained, respectively, by structures in which all aromatic rings are immobile, only the phenylene rings are rotating, and all rings are undergoing rapid rotational motion. However, the computer models required a much larger distribution of angles between the polymer chain axes and the draw axis of the sample than expected on the basis of qualitative inspection of the X-ray diffraction patterns.

Although we have at present no quantitative measure of molecular orientation by X-ray diffraction in the samples we have studied, work on drawn fibres of monomer ratio 73:27 at ambient temperatures has yielded $\langle P_2(\cos(\Delta))\rangle = 0.90$ and $\langle P_4(\cos(\Delta))\rangle = 0.89$ (ref. 5).

The availability of a Bruker MSL-300 *FT*n.m.r. spectrometer has made it possible to obtain data of greater resolution than has hitherto been possible with the CW spectrometer. We have, therefore, extended the studies to the 30:70 ratio material and in addition included further measurements on the 73:27 version.

EXPERIMENTAL

Materials

Two copolymers prepared from 4-hydroxybenzoic acid and 2-hydroxy-6-naphthoic acid (*Figure 1*) were supplied by the Celanese Research Company, Summit, New Jersey, USA. The two monomers, as they appear in the copolymer chain, are shown in *Figure 1*. They have monomer ratios (HBA:HNA) of 73:27 and 30:70 and will be referred to as HBA rich and HNA rich, respectively. Samples were in the form of strips approximately 3 mm wide and 0.1 mm thick for the HBA rich material and 0.05 mm thick for the HNA rich material. They had been produced by spinning a thin tape with a high draw down, followed by annealing at constant length in a nitrogen atmosphere for 4 h at 250°C and then 15 h at 280°C. Examination of the samples by wide angle X-ray diffraction showed that they possessed a high degree of molecular orientation.

N.m.r. measurements

Proton n.m.r. spectra were obtained using a Bruker MSL 300 spectrometer fitted with a high power proton probe. Radio frequency power was chosen to yield a proton 90° pulse length of 1 μs. Recycle delay times varied from 75 s at −100°C to 30 s at 150°C. A major problem in pulsed n.m.r. spectroscopy of solids is receiver dead time at around $t=0$ s. The approach taken to overcome this was to extrapolate the time domain signal back to $t=0$ s with a polynomial function.

Samples for use in the n.m.r. spectrometer were prepared by stacking 4 mm lengths of the highly oriented

---

* To whom correspondence should be addressed

0032-3861/91/0200202-07

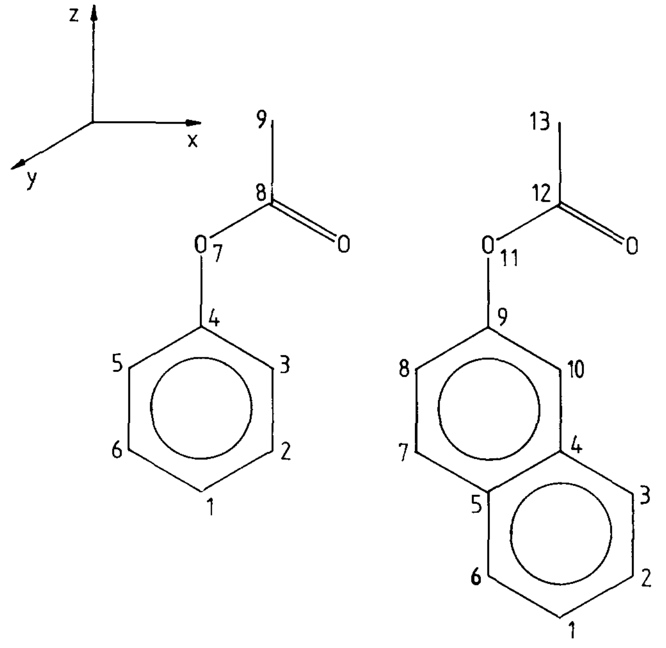

Figure 1 The HBA and HNA units, from which the copolymers are constructed

strips, with their draw axes parallel to one another, into a PTFE holder. The PTFE holder was mounted into the high power proton probe of the Bruker MSL 300 n.m.r. spectrometer with the sample axis at known angles relative to the spectrometer magnetic field B_0.

Dynamic mechanical studies[3] at frequencies from 10^{-2} to 10 Hz have yielded transition maps for the two copolymers studied here. Extrapolation of the data to the n.m.r. spectrum linewidth ($\approx$300 000 Hz) indicates that motional narrowing due to HBA rotations should be observed at $\approx$20°C and for the HNA rotations at $\approx$150°C. However, for the HNA rich material the onset of rapid HNA group motion lies relatively close to 150°C. This is the recommended upper temperature limit of our n.m.r. probe. At −100°C the sample should behave as a rigid lattice. Proton spectra of the copolymer materials were, therefore, initially obtained at −100, 20 and 150°C. Subsequent comparison of experimental and model data caused us also to record spectra of the HBA rich material at 100°C. At each of these temperatures, spectra were recorded with the sample axes oriented at 15° intervals between 0 and 90°.

THEORY

McBrierty and Ward[6] have shown that transversely isotropic oriented materials have n.m.r. second moment anisotropies that may be expressed in terms of Legendre functions as follows:

$$\langle \Delta H^2 \rangle = \sum_{l=0,2,4} A_l P_l(\cos(\gamma))P_l(\cos(\Delta))$$

where:

$A_0 = (4/5)G(4\pi)^{1/2}S_{00}$;
$A_2 = (8/7)G(4/5\pi)^{1/2}S_{20}$;
$A_4 = (72/35)G(4/9\pi)^{1/2}S_{40}$;
$G = (3/4)[I(I+1)g^2\mu_n^2]$;

$S_{l0} = (1/N)\sum_{j>k} r_{jk}^{-6}\gamma_{l0}(\theta_{jk}, \Phi_{jk})$;
$\gamma_{l0} = [(2l+l)/(4\pi)]^{1/2}P_l(\cos(\theta_{jk}))$

and P_l are Legendre functions. In these equations, I is the nuclear spin quantum number, g is the nuclear g factor and μ_n is the nuclear magneton. The lattice sums S_{l0} are functions of the inter-proton separations r and the angles θ they make relative to the spectrometer field B_0. Terms $P_l(\cos\gamma)$ determine the angular dependence of the second moment upon the angle γ that the sample draw axis makes relative to the spectrometer field B_0. Terms $P_l(\cos\Delta)$ introduce an angular distribution of chain axes about the sample draw axis.

If HBA or HNA groups are undergoing rapid rotation in the copolymer, then the dipolar interactions must be averaged over the motion[7]. This involves projecting the coordinates of protons on mobile groups onto the axis of rotation before calculating the dipolar interactions. The axes of rotation that have been investigated will be described in the next section.

COMPUTER MODELLING

The major part of modelling the copolymer second moment anisotropies was concerned with constructing feasible structural models and then using them to calculate the lattice sums S_{l0}. The structural models were based upon those used by Biswas and Blackwell[2] and Windle[8] to simulate X-ray diffraction data.

Copolymer chains were built up from random sequences of dimers formed from the HBA and HNA groups. Three types of dimer are possible and are listed in *Table 1* along with the fractional contents, calculated by using simple binomial statistics, found in each of the materials studied. The two ester linkages in each dimer were oriented in opposite directions, as shown in *Figure 2*, in order to obtain approximately linear copolymer chains. A non-zero dihedral angle between the groups was formed by rotating them in opposite directions about

Table 1 Three possible types of dimer and their fractional content in the copolymers

Type of dimer	73:27	30:70
HBA:HBA	0.5329	0.0900
HBA:HNA	0.3942	0.4200
HNA:HNA	0.0729	0.4900

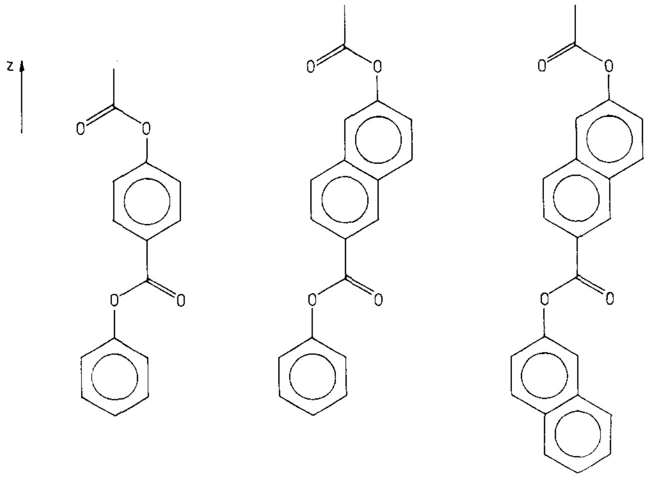

Figure 2 The three types of dimer from which the model copolymer materials were constructed

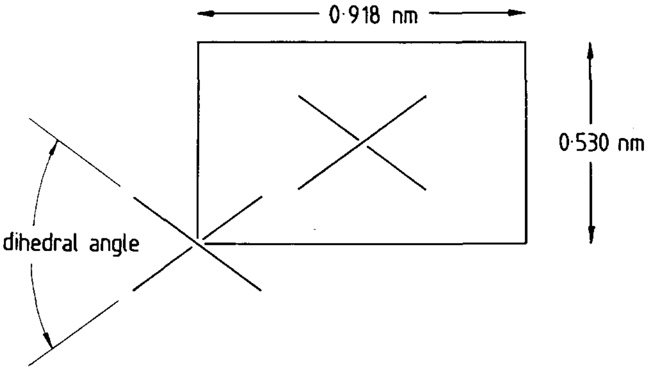

Figure 3 Schematic representation of the orthorhombic unit cell at the centre of the model copolymer structure and the arrangement of dimers within it

axes parallel to the z-axis and passing through the aromatic ring carbons attaching them to the carbon atom in the ester links.

Two complementary copolymer chains were constructed. One chain was formed from mirror image dimers, reflected in the y, z plane, of those used to build the other chain. These two chains were brought together so that the central dimers formed the orthorhombic unit cell of dimensions $0.918 \times 0.530\ \mathrm{nm}^2$ (*Figure 3*) that is deduced from X-ray diffraction data. These lattice dimensions relate to disordered chain packing known to exist in pre-annealed samples. X-ray diffraction has shown that our samples are predominantly of this form. Such chain pairs were then packed together to form models of the copolymer structures. Adjacent chains formed a pseudo-hexagonal lattice at their centres but increasingly lost this order upon moving along the chain. This effect was not severe within a sphere of radius 0.20 nm centred on the structures central dimer pair. Second moments are dependent upon an r^{-6} relationship between interacting protons and it is found that little advantage is obtained by considering proton–proton separations >0.20 nm.

Each type of unit cell was placed in turn at the centre of the copolymer chains and, therefore, at the centre of the model lattice. Lattice sums were calculated from interactions between protons within the central unit cell and also between the central unit cell and all other dimers in the structure. The lattice sums were then weighted according to the fractions of dimers in the sample and the results added before calculating the second moment.

To match model second moment anisotropy curves to experimental data a number of parameters were allowed to vary. The dihedral angle between groups in a dimer was the main influence upon the values obtained. A smaller effect was derived from translating chains at the edges and centres of the unit cells relative to one another and parallel to the chain axis. Angular distributions of chain axes about the draw axes were introduced to allow for less than ideal alignment in the sample.

Each type of group could also be given rapid rotational motion independently of the other. Four rotation axes were investigated, each having an aromatic carbon bound to an ester link as one end point (atoms 1 in *Figure 1*) and an atom in the adjacent linkage on the same chain as the other end point (HBA atoms 4, 7–9 and HNA atoms 9, 11–13 in *Figure 1*). Second moment anisotropy curves were calculated for structures possessing groups having the following mobilities:

(1) rigid lattice;
(2) HBA groups rotate rapidly; and
(3) HBA and HNA groups rotate tapidly.

Previous dynamic and dielectric relaxation studies have shown that the smaller HBA groups became mobile before the HNA groups as temperature is raised. The possibility of HNA groups only being mobile is therefore omitted from the preceding list.

Comparison of model and experimental second moment anisotropies proceeded in two stages. First the model structure was varied to find the best fit to the experimental isotropic second moment A_0 and then the angle Δ which describes the orientation functions $P_l(\cos\Delta)$ was varied to minimize the r.m.s. deviation between the second moment lineshapes.

RESULTS AND DISCUSSION

Examples of the proton n.m.r. spectra obtained from the two copolymers are given in *Figures 4* and *5*. That of the HBA rich material approximates to a doublet, while the HNA rich material gives a spectrum that is better described as a triplet.

The form of these spectra may be accounted for by considering nearest neighbour interactions between protons. These occur between protons on the same side of any given aromatic ring. In the highly oriented materials reported here, all the inter-proton vectors between nearest neighbours are approximately parallel to one another and to the draw axis. On an HBA ring there are

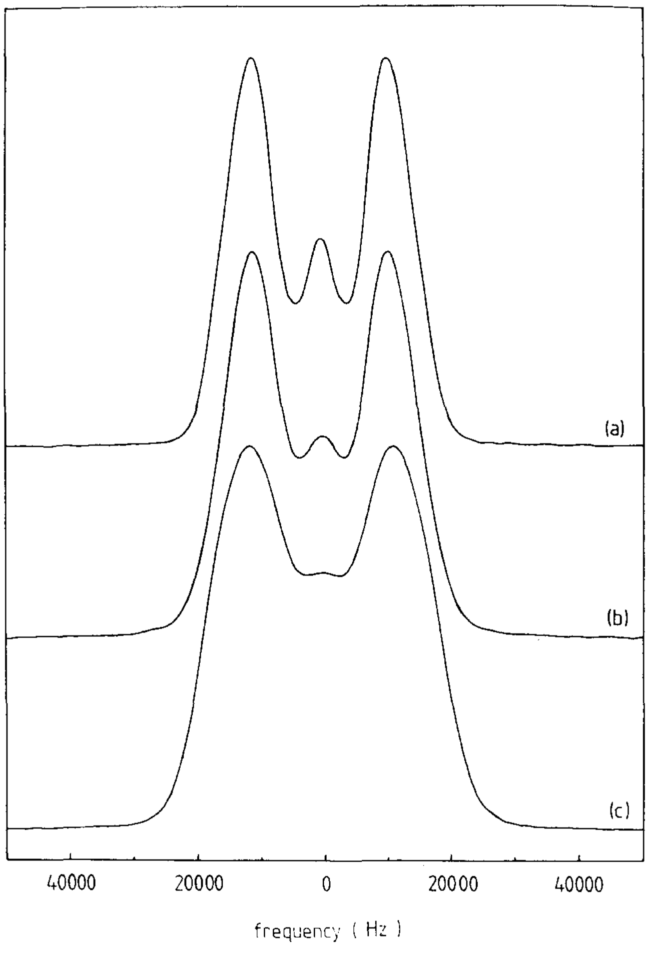

Figure 4 Experimental proton n.m.r. spectra from the HBA rich material, for $\gamma = 0$: (a) 150°C; (b) 100°C; (c) −100°C

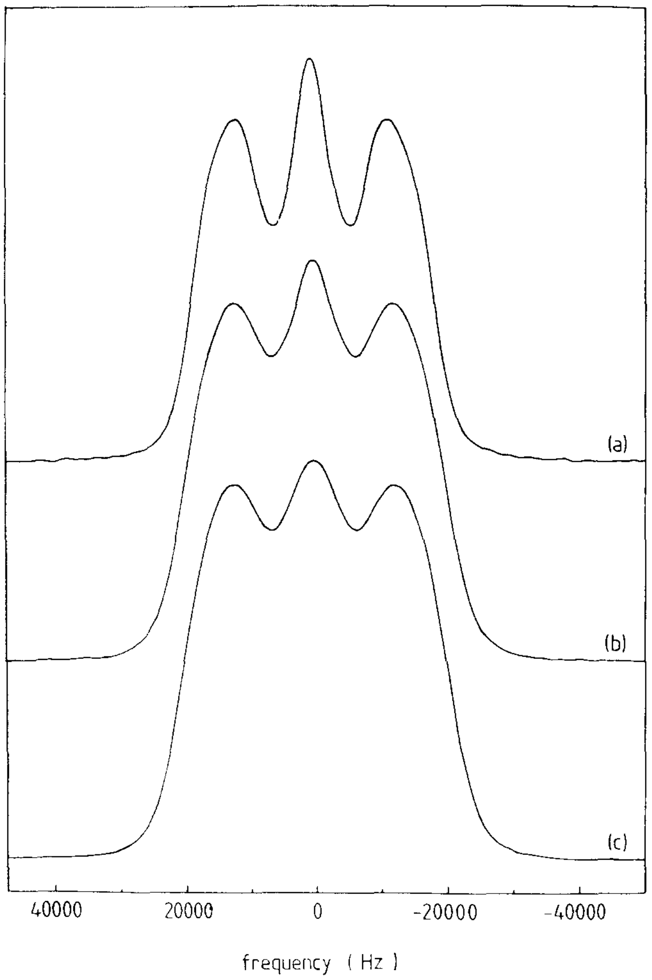

Figure 5 Experimental proton n.m.r. spectra from the HNA rich material, for $\gamma = 0$: (a) 150°C; (b) 20°C; (c) −100°C

two nearest neighbour protons attached to carbons 2 and 3 on one side and to carbons 5 and 6 on the other (see *Figure 1*), giving rise to a doublet component in the spectra. On an HNA unit there are three protons on the same side of any given ring. The outer protons (for instance the protons attached to carbons 2 and 10) essentially have only the central proton attached to carbon 3 as a nearest neighbour, the other proton being relatively far away, due to the r^{-3} dependence of the dipole interaction. The outer protons on an HNA ring, therefore, give rise to a doublet component in the proton spectrum. The inner proton (for example, attached to carbon 3), however, has two nearest neighbours (attached to carbons 2 and 10) and produces a triplet component in the proton spectrum. In the HBA rich material there are only 27% of rings that can contribute a triplet to the spectrum, whereas in the HNA rich version 70% of all rings can supply a triplet component. Hence the stronger triplet nature of the HNA rich material as opposed to the doublet of the HBA rich copolymer.

Longer range interactions are not observed as individual features in the spectra, but give rise to the relatively large halfwidths (≈ 14000 Hz) of the individual peaks. This makes it difficult to separate the contributions to the lineshapes from the HBA and HNA groups. It also complicates interpretation of any simple changes in the spectra due to temperature variation (such as the principle dipolar splitting), since either changes in peak positions or linewidths, or a combination of both may give rise to the observed effect.

Because of the difficulty in studying individual features of the n.m.r. spectra, we have concentrated on modelling their second moment values. These are essentially the normalized moment of inertia of the spectrum, calculated parallel to the frequency axis. Second moments were evaluated as a function of angle γ between the sample draw axis and the spectrometer magnetic field B_0 at several different temperatures. The experimental points are shown in *Figures 6* and *7* along with curves fitted by the least squares method to the function

$$H^2 = A_0P_0(\cos\gamma) + A_2P_2(\cos\gamma) + A_4P_4(\cos\gamma)$$

where P_0, P_2 and P_4 are Legendre functions. Values of the isotropic second moments are given in *Table 2*.

Model second moment anisotropy curves corresponding to the experimental curves are shown in *Figures 8* and *9*. The isotropic second moments (A_0) are given in *Table 3* for comparison with the experimental values in *Table 2*. We shall discuss the matches between model and experimental data obtained from the two copolymer materials separately.

For the HBA rich material, the experimental second moment anisotropy curve obtained at −100°C can be modelled successfully by a lattice containing aromatic rings possessing no rotational freedom. At 150°C, the opposite extreme is encountered, where all the aromatic rings appear to be undergoing rapid rotational motion. The results obtained at these temperatures were expected on the basis of the transition map given in Reference 3. However, the model anisotropy curve for a system of

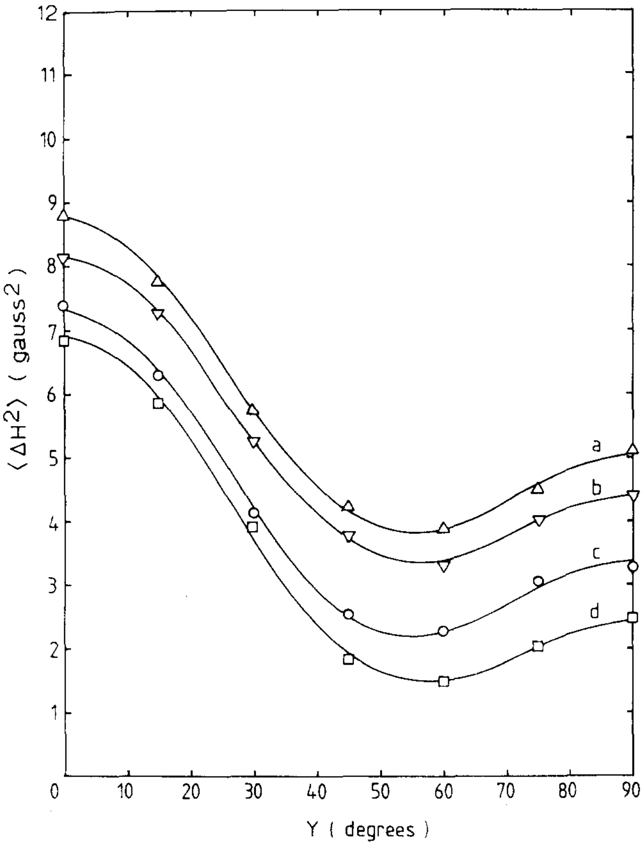

Figure 6 Experimental proton n.m.r. second moment anisotropies from the HBA rich material at: (a) −100°C; (b) 20°C; (c) 100°C; (d) 150°C

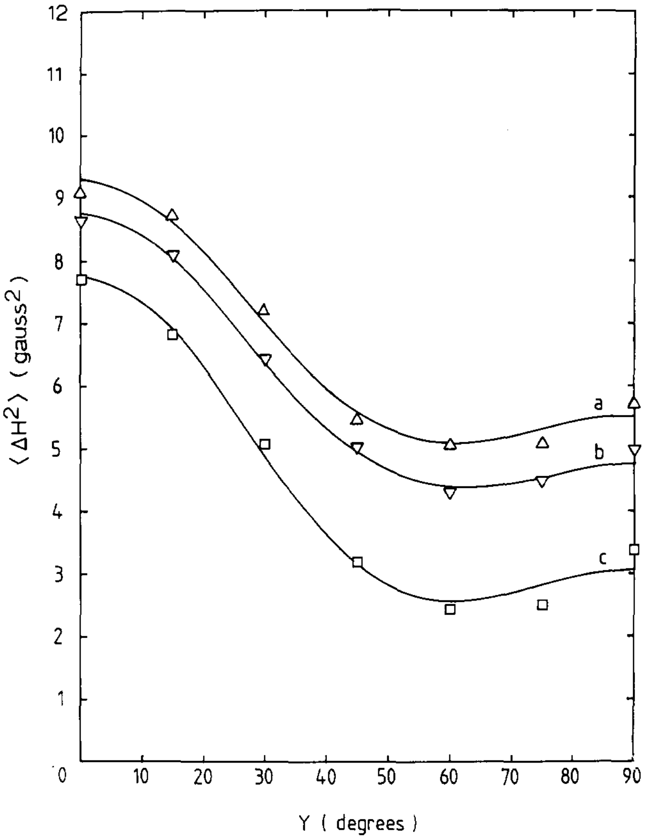

Figure 7 Experimental proton n.m.r. second moment anisotropies from the HNA rich material at: (a) −100°C; (b) 20°C; (c) 150°C

Table 2 Experimental isotropic second moments A_0 (G^2) obtained from the two copolymers

Temperature (°C)	73:27	30:70
−100	4.80	5.79
20	4.27	5.11
100	3.19	–
150	2.50	3.42

rapidly rotating HBA rings and immobile HNA rings is not matched by the experimental curve until a temperature of ≈100°C is achieved. Certainly, the change in the experimental curve between −100 and 20°C is not consistent with 73% of all available aromatic rings acquiring rapid rotational motion.

Turning now to the HNA rich material, we again find that the experimental anisotropy curve observed at −100°C is consistent with a rigid lattice of aromatic rings. The experimental curve obtained at 20°C is compatible with model data for rapidly rotating HBA rings and immobile HNA rings. This is now in agreement with the transition map of Reference 3. At 150°C, comparison of the experimental and model curves suggests that all aromatic rings are not yet mobile. It has already been mentioned that at n.m.r. linewidths the onset of rapid rotational motion of the HNA groups lies relatively close to 150°C. The higher temperature for the α (glass) transition and β transition (associated with rotational motion of the HNA groups) is consistent with the transition map derived from tensile data, which shows the same trend. The temperature of 150°C is the recommended upper operating limit of the n.m.r. probe and has not yet been exceeded.

The values of the parameters required to generate the model curves are similar for both versions of the copolymer that have been examined and are as follows:

(1) For the cases where adjacent groups on the same polymer chain do not rotate relative to one another, the dihedral angles between the planes of the aromatic rings is 70–74°. These values are consistent with those reported by Windle[8] after examination of crystallographic data from a variety of related compounds.

(2) Where rapid rotation of the groups occurs, the choice of rotation axis makes little difference to the anisotropy curve obtained. For the four rotation axes investigated, the spread of isotropic second moment values is $\pm 0.03\ G^2$.

(3) Chains at the corners and at the centres of the unit cells are translated parallel to the chain axis by 0.14 to 0.16 nm relative to one another. Biswas and Blackwell[2] have already reported that a distribution in chain register, with standard deviation of 0.2 nm, must be allowed to simulate X-ray diffraction patterns.

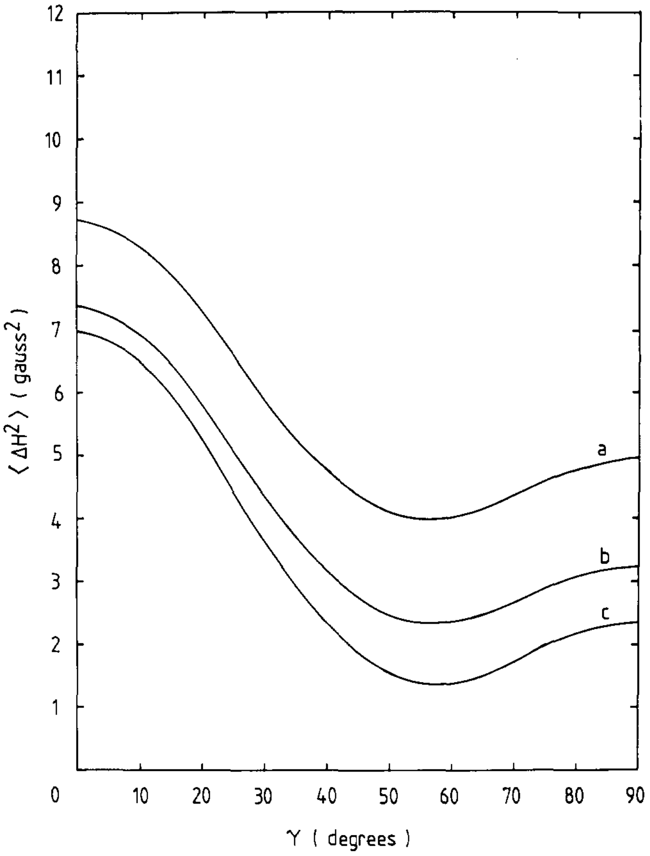

Figure 8 Model proton n.m.r. second moment anisotropies for the HBA rich material for: (a) rigid lattice; (b) HBA rings only mobile; (c) HBA and HNA rings mobile. Values of $\langle P_2(\cos(\Delta))\rangle$ and $\langle P_4(\cos(\Delta))\rangle$ used to describe the distribution of chain axes are given in *Table 4*

Table 3 Model isotropic second moments A_0 (G^2) obtained by optimizing the structural parameters in the computer model

Group mobility			
HBA	HNA	73:27	30:70
No	No	4.84	5.69
Yes	No	3.22	5.04
Yes	Yes	2.41	2.59

Table 4 Values of Legendre functions required to give best fit between experimental and model second moment anisotropy curves

	73:27		30:70	
Temp (°C)	$\langle P_2(\cos(\Delta))\rangle$	$\langle P_4(\cos(\Delta))\rangle$	$\langle P_2(\cos(\Delta))\rangle$	$\langle P_4(\cos(\Delta))\rangle$
−100	0.90	0.89	0.96	0.87
20	–	–	0.93	0.78
100	0.85	0.69	–	–
150	0.83	0.65	0.83	0.65

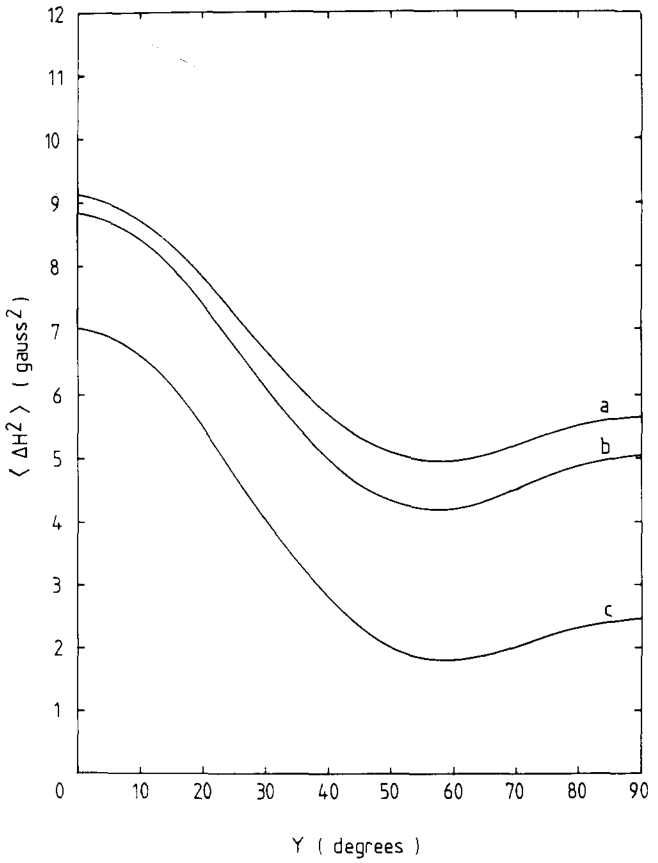

Figure 9 Model proton n.m.r. second moment anisotropies for the HNA rich material for: (a) rigid lattice; (b) HBA rings only mobile; (c) HBA and HNA rings mobile. Values of $\langle P_2(\cos(\Delta))\rangle$ and $\langle P_4(\cos(\Delta))\rangle$ used to describe the distribution of chain axes are given in *Table 4*

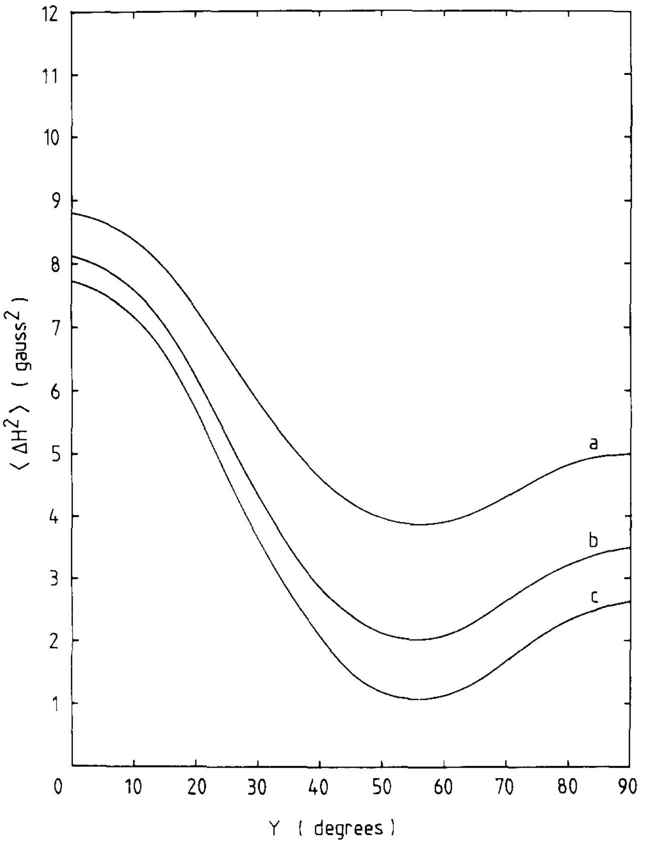

Figure 10 Model proton n.m.r. second moment anisotropies for the HBA rich material for: (a) rigid lattice; (b) HBA rings only mobile; (c) HBA and HNA rings mobile. Rigid lattice values of $\langle P_2(\cos(\Delta))\rangle = 0.90$ and $\langle P_4(\cos(\Delta))\rangle = 0.89$ have been used for all three curves

(4) The values of $\langle P_2(\cos(\Delta))\rangle$ and $\langle P_4(\cos(\Delta))\rangle$ used in the orientation functions to generate the model second moment anisotropy curves in *Figures 8* and *9* are given in *Table 4*. These values indicate a high degree of molecular orientation which is consistent with qualitative inspection of the X-ray diffraction patterns and the aggregate modelling of the mechanical behaviour. The latter does, however, assume that $\langle P_2(\cos(\Delta))\rangle$ is a constant at all temperatures. In the n.m.r. studies reported here the fits between experimental and model anisotropy curves are substantially improved if the angular distribution of chain axes relative to the draw axis is allowed to increase with temperature. This is qualitatively consistent with the negative thermal expansion coefficient[9] that these materials are known to have parallel to the draw axis.

The model anisotropy curves obtained by applying the values of $\langle P_2(\cos(\Delta))\rangle$ and $\langle P_4(\cos(\Delta))\rangle$ found at −100°C to higher temperatures are given in *Figures 10* and *11*. For the HBA rich material it can be seen directly that the fits to the experimental curves of *Figures 6* and *7* are poorer than when the orientation functions are allowed to vary. For the HNA rich material, no direct comparison is possible at 150°C, but it is found that the curves are made approximately parallel by decreasing the values of $\langle P_2(\cos(\Delta))\rangle$ and $\langle P_4(\cos(\Delta))\rangle$ (compare *Figures 7* and *9*). This is the more plausible fit because there are aromatic rings yet to become mobile at higher temperatures and a further drop in the second moments is expected at all sample orientations γ relative to the spectrometer field B_0.

CONCLUSIONS

Highly oriented tapes of HBA:HNA copolymers yield large anisotropies in the second moments of their proton n.m.r. lineshape. This anisotropy also changes markedly with temperature. Using computer models of the copoly-

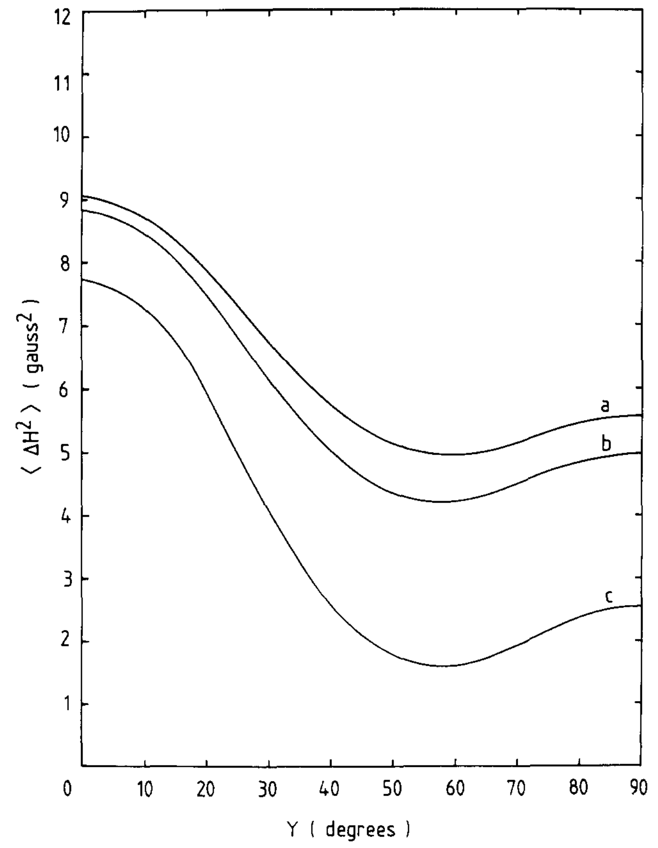

Figure 11 Model proton n.m.r. second moment anisotropies for the HNA rich material for: (a) rigid lattice; (b) HBA rings only mobile; (c) HBA and HNA rings mobile. The rigid lattice values of $\langle P_2(\cos(\Delta))\rangle = 0.96$ and $\langle P_4(\cos(\Delta))\rangle = 0.87$ have been used for all three curves

mer structures, we have shown that the experimental anisotropies are consistent with chains placed on a pseudo-hexagonal lattice.

At −100°C the lattices are rigid and aromatic rings on adjacent chains assume an edge to face configuration. Such nearest neighbour chains require an offset relative to one another and parallel to the chain axes of ≈ 0.15 nm. Dihedral angles between adjacent rings on the same chain of ≈ 70–$74°$ are necessary. At 150°C all aromatic rings in the HBA rich material appear to have rotational freedom, while in the HNA rich version there is evidence for a fraction of the rings still being relatively immobile. The temperatures at which all HBA rings may be considered to be mobile and the HNA rings immobile are 100 and 20°C for the HBA rich and HNA rich materials, respectively.

We speculate here upon the reasons for the different molecular dynamic behaviour between the two copolymer materials. The version with a majority of the smaller HBA units may be expected to have closer packed chains than the version containing a majority of the larger HNA units. Motion of the HBA groups may, therefore, be sterically hindered to a greater extent in the HBA rich material than in the HNA rich material. Where the larger HNA groups dominate the chain packing the smaller HBA groups may experience relatively greater free volume in which rapid rotational motion can take place. This may account for the lower temperature (20°C) at which all the HBA groups may be considered to be undergoing rapid rotational motion in the HNA rich material, relative to the HBA rich material (100°C). When the temperature is raised, the HNA groups may rotate more freely in the HBA rich material, where there is a greater probability of being surrounded by already rapidly rotating HBA groups, than in the HNA rich material, where the probability is higher of being surrounded by other still relatively immobile HNA groups. This would explain the observed lower temperature for rapid HNA motion in HBA rich material.

To account fully for the experimental second moment anisotropies, distributions of chain axes about the draw axis are necessary. The values of $\langle P_2(\cos(\Delta))\rangle$ and $\langle P_4(\cos(\Delta))\rangle$ required confirm that the samples are highly oriented. There does, however, appear to be a moderate reduction in the degree of order as temperature is increased, probably due to increasing chain motion. The n.m.r. dipolar interaction is a relatively short range interaction. The increase in the orientation functions with temperature may, therefore, only indicate local disordering of the chains. The larger scale alignment of the polymer chains need not change.

In our modelling of the HBA:HNA copolymers we have assumed that the aromatic rings and ester linkages rotate in unison. This was for convenience only and the relationship between rings and linkages during motion remain unresolved. However, preliminary results of ^{13}C-MAS n.m.r. spectra are encouraging and show that the aromatic rings and ester linkages can be studied separately. Furthermore, selectively deuterated samples have been prepared and are further assisting our investigations into this family of materials. We are, therefore, optimistic that n.m.r. spectroscopic studies of the HBA:HNA copolymers will considerably advance our knowledge of their dynamic and structural properties.

ACKNOWLEDGEMENTS

We thank the Celanese Research Company, Summit, New Jersey, USA for providing the highly oriented tapes.

REFERENCES

1 Davies, G. R. and Ward, I. M. 'High Modulus Polymers – Approaches to Design and Development' (Eds. A. E. Zachariades and R. S. Porter), Marcel Dekker, New York, 1988, pp. 37–69
2 Biswas, A. and Blackwell, J. *Macromolecules* 1988, **21**, 3146–3164
3 Troughton, M. J., Davies, G. R. and Ward, I. M. *Polymer* 1989, **30**, 58
4 Clements, J., Humphreys, J. and Ward, I. M. *J. Polym. Sci., B, Polym. Phys.* 1986, **24**, 2293–2305
5 Karacan, I. Private communication, 1990
6 McBrierty, V. J. and Ward, I. M. *J. Phys. D* 1968, **1**, 1529
7 Gutowsky, H. S. and Pake, G. E. *J. Chem. Phys.* 1950, **18**, 162
8 Windle, A. H. Private communication, 1989
9 Green, D., Orchard, G. A. J., Davies, G. R. and Ward, I. M. *J. Polym. Sci. B, Polym. Phys.* in press